CrossMark

ORIGINAL RESEARCH

Nucleophilic properties of purine bases: inherent reactivity versus reaction conditions

Anna Stachowicz-Kuśnierz[1] · Jacek Korchowiec[1]

Abstract In the present study, nucleophilic properties of adenine and guanine are examined by means of density functional theory. H^+ is used as a model electrophile. Two modes of H^+ attack on the bases are considered: on the neutral molecule and on the anion. Solvent effects are modeled by means of polarizable continuum model. Regioselectivity of attack is studied by analyzing two contributions. The first one is the energetic ordering of the tautomers. The second is the relative inherent reactivity of nucleophilic sites in the bases. Atomic softnesses calculated by means of charge sensitivity analysis are employed for this purpose. The most reactive sites in various tautomers are identified on the ground of Li–Evans model. For adenine, it is demonstrated that both in basic and in neutral pH *N7* atom possesses the most nucleophilic character. In polar solvents, *N7* substitution is also most favored energetically. In basic pH and nonpolar solvents as well as in the gas phase, *N9* substitution is slightly more probable. For guanine, a mixture of *N7*- and *N9*-substituted products can be expected in basic pH. In neutral pH, inherent reactivity and energy trends are opposite to each other; therefore, the substitution does not occur. Experimentally observed products of reactions with various electrophiles and in various conditions confirm the results obtained in this study.

Keywords Purine bases · Electrophilic attack · Solvent effects · Reactivity indices · Fukui function

Introduction

Electrophilic attack on nucleobases is a common molecular mechanism of mutagenicity or carcinogenicity [1, 2]. It is involved in deleterious properties of many mutagens starting with environmental pollutants [3, 4] to finish with endogenous substances or their metabolites [5, 6]. Adduct formation can lead to perturbations in hydrogen-bonding (HB) pattern, conformational interconversions, formation of interstrand cross-links [7–9] or abasic sites [10] and in consequence to nucleic acids' malfunction or damage.

Similar to most biological processes, regioselectivity plays an important role here. It is governed by either kinetic or thermodynamic factors [11]. The first ones are connected with relative heights of activation barriers. In the latter, stability of the products is decisive. In both cases, the observed trends can arise from two sources. One is the inherent reactivity of various sites. It arises from electronic structure of the reagent and is independent of the reaction partner. It is believed that the most nucleophilic atoms of purines are the *N7* atom of guanine and *N1* atom of adenine (IUPAC atoms numbering; see Figs. 1, 2). In this respect, hard and soft acids and bases (HSAB) theory [12, 13] is often invoked along with the empirical Kornblum's rule [14] and Klopman's model of charge- and orbital-controlled reactions [15]. The other sources are connected with various specific interactions between the reagents and/or

✉ Anna Stachowicz-Kuśnierz
stachowa@chemia.uj.edu.pl

[1] K. Gumiński Department of Theoretical Chemistry, Faculty of Chemistry, Jagiellonian University, R. Ingardena 3, Kraków, Poland
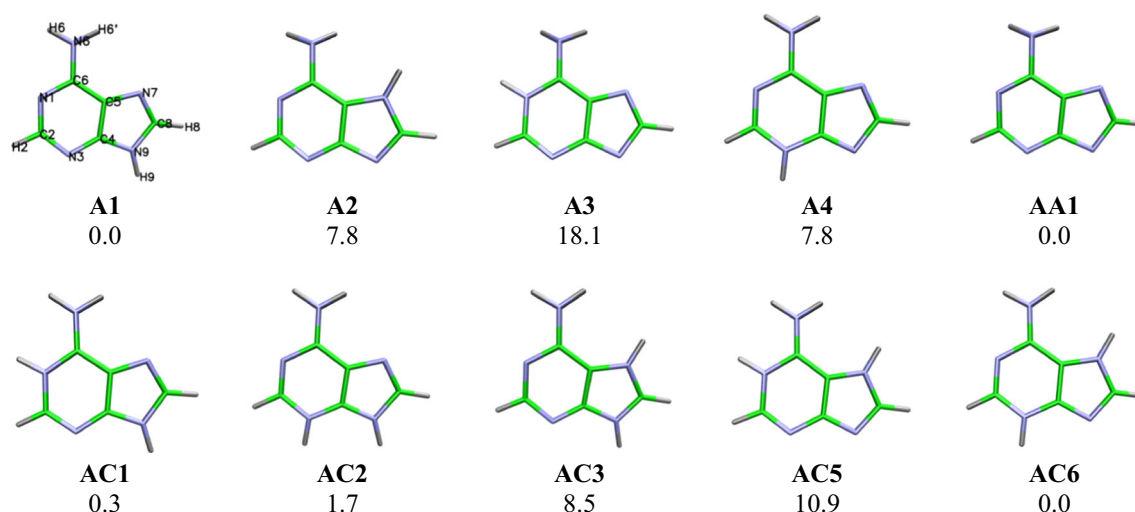
Fig. 1 Optimized gas phase structures of isomers of adenine and its ions with their DFT/B3LYP/6-31+G(3df,2p) (kcal/mol) energies relative to the lowest-energy forms **A1**, **AA1** and **AC6**

the environment. These include the following: solvent effects [16, 17], solvent-assisted reaction mechanisms [18, 19], the influence of pH on ionic equilibriums [20–24] or specific interactions between reagents, in particular HBs and steric interactions [19, 25].

Due to this manifold of factors, computational modeling is a particularly advantageous tool in this field, allowing for separation of different contributions to observed trends. For example, Ford and Scribner [26] have used MNDO calculations in studies of nucleobases' alkylation by alkylnitrosoureas. They have shown that optimal geometry of the transition state determines the preferences for either oxygen or nitrogen attack by these agents. Freccero et al. [19] have employed density functional theory (DFT) [27] in studies of adenine and guanine alkylation by quinone methide. They have demonstrated that the unusual preference of this agent to alkylate weakly nucleophilic exocyclic amine groups is due to its ability to form HBs with the nucleobases. Also on the basis of DFT calculations, the group of Mavri and Bren has confirmed the S_N2 mechanism proposed for reaction of purines with epoxides [28, 29]. Another studies concerning, e.g., ionic equilibriums in aqueous environment [30], optimal structures of the adducts and their biological implications [8, 25] or the mutual influence of base pairing and adduct formation [31, 32] have also been pursued.

All of the above studies are based on considering the energetic effects of the examined reactions. However, DFT has recently witnessed a great progress in its conceptual branch [33]. It tackles the problem of chemical reactivity by employing a perturbative approach, similar to experimental thermodynamics [34]. A lot of properties

known from experimental chemistry, such as chemical potential, electronegativity, polarizability or hardness and softness, can be given strict definitions on the ground of conceptual DFT. Other reactivity descriptors, e.g., Fukui function [35] or various electrophilicity/nucleophilicity indices [36–38] can also be defined. They have been successfully applied in modeling various reactions [33, 39], and lately also chemical toxicity [40].

In our group, a method called charge sensitivity analysis (CSA) has been developed [41]. It is derived from DFT and was originally formulated to extract chemically relevant information from ab initio calculations in different resolutions. We have recently parameterized its semiempirical variant in force-field atoms resolution [42, 43]. It allows efficient calculating of equilibrium charge distribution and a set of reactivity indices by a single matrix inversion step. In the present study, we demonstrate the usefulness of this approach in description of nucleophilic properties of purines. We combine CSA reactivity descriptors with energetic considerations in various solvents in order to separate the contribution of inherent reactivity and reaction conditions to observed regioselectivity. Another goal of this study is to verify the agreement of the obtained reactivity parameters with experimental results before moving on to large biological systems. Complexity of purines' electronic structure should provide a sufficiently challenging test for the method.

The paper is organized as follows. In the next section, a short overview of CSA formalism is presented. Next, computational details are given, followed by "Results and discussion" section. The last section contains conclusions and some future prospects.
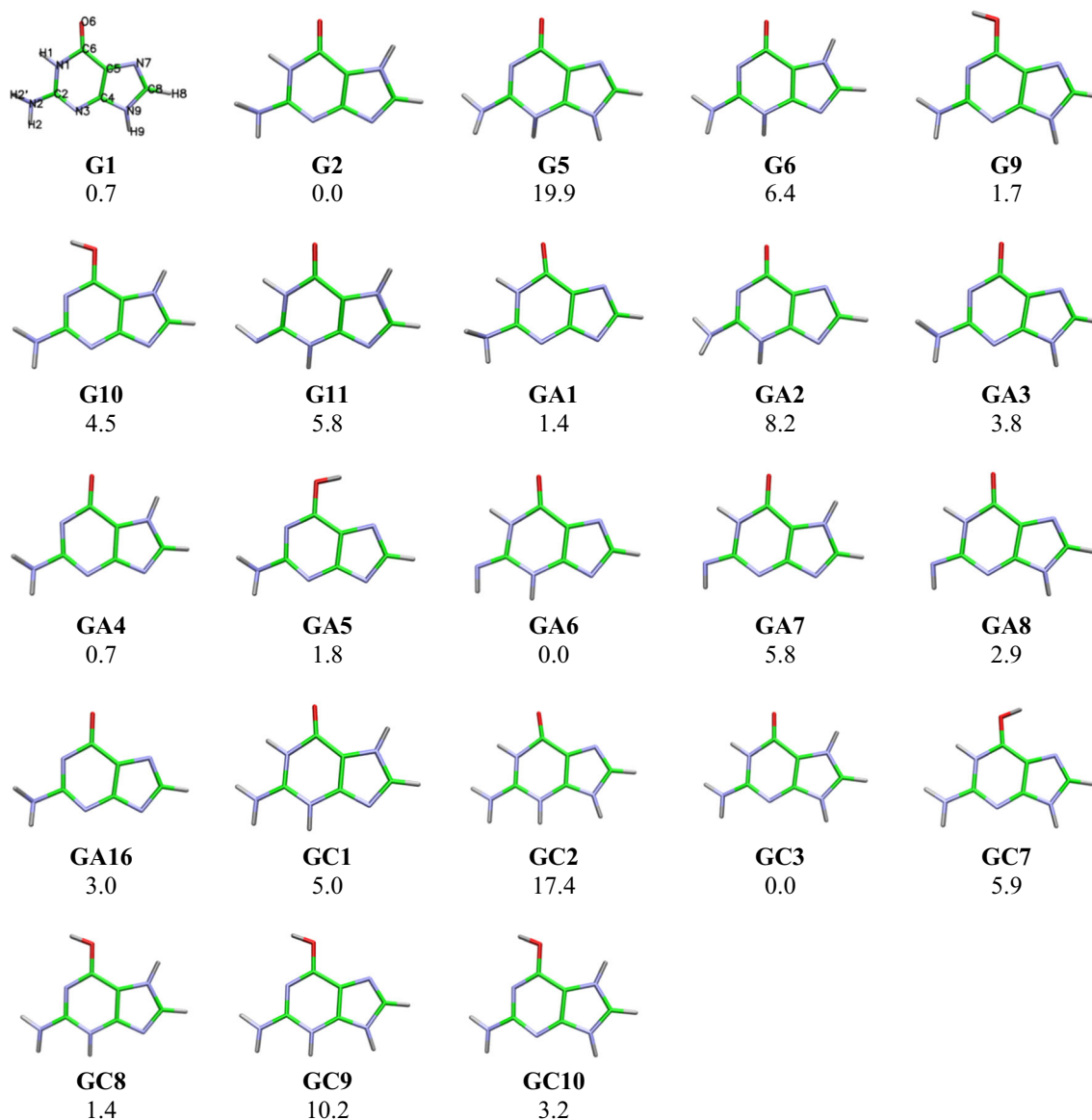
Fig. 2 Optimized gas phase structures of isomers of guanine and its ions with their DFT/B3LYP/6-31+G(3df,2p) (kcal/mol) energies relative to the lowest-energy forms **G2**, **GC3**, **GA6** and **GA17**

Theoretical background

Conceptual DFT approach to chemical reactivity resembles that of phenomenological thermodynamics. The behavior of the system is described in terms of its responses (sensitivities) to perturbations in state parameters. In studies of chemical reactivity, these usually are the number of electrons, N, and the external potential due to nuclei, $v(r)$. Perturbation in N corresponds to oxidation/reduction of the molecule. Change in $v(r)$ models the presence of the other reagent. By expanding the system's energy, E, in a second-order Taylor series with respect to these variables, a number of sensitivities can be defined. They include the global chemical potential of electrons (μ) [44], the global

hardness (η) [45], polarization/linear response kernel (β) [46] and Fukui function ($f(r)$) [47].

Chemical potential μ measures the leaving tendency of electrons in the system. For systems in the state of global equilibrium, it is equalized through space [48–50]. Global hardness describes the system's resistance on charge flow. It depends on its global charge, size and polarizability [51, 52]. It is directly linked with the concept of chemical hardness and softness in HSAB principle [53–55]. The inverse of the global hardness is the global softness, S. Polarization/linear response kernel measures the response of electron density in position r to perturbation of external potential in position r'. It can be used to probe various properties of molecular systems, such as electron delocalization, aromaticity/

antiaromaticity and other aspects of organic/inorganic/metallic chemistry [56–59]. Finally, Fukui function is a local property describing the response of electron density, $\rho(\boldsymbol{r})$, to oxidation/reduction of the system. It is defined as:

$$f(\boldsymbol{r}) \equiv \frac{\partial}{\partial N}\left(\frac{\delta E}{\delta v(\boldsymbol{r})}\right) = \left(\frac{\partial \rho(\boldsymbol{r})}{\partial N}\right)_{v(\boldsymbol{r})} = \left(\frac{\delta \mu}{\delta v(\boldsymbol{r})}\right)_N \quad (1)$$

It can be regarded as a measure of local reactivity: The sites of maximum $f(\boldsymbol{r})$ should correspond to maximum sensitivity to electrophilic/nucleophilic attack. $f(\boldsymbol{r})$ is normalized to unity. It can be shown [35] that a quantity called the local softness, defined as $s(\boldsymbol{r}) = (\partial \rho(\boldsymbol{r})/\partial \mu)_{v(\boldsymbol{r})}$, can be calculated with the use of $f(\boldsymbol{r})$:

$$s(\boldsymbol{r}) = f(\boldsymbol{r})S \quad (2)$$

A systematic approach to compute these quantities is offered by CSA. The details of this formalism can be found in the literature [41, 42, 60]. Here, only a short overview is given. In CSA, a molecular system M is divided into either mutually closed or opened subsystems. The number of electrons in each subsystem can be controlled by coupling it to a hypothetical external reservoir of electrons with constant chemical potential. Mutually opened subsystems are coupled to the same reservoirs. Consider, for example, a reaction between a Lewis acid, A, and base, B:

$$A \quad + \quad :B \rightarrow A:B \quad (3)$$

In the early stages of the reaction fragments, A and B can be regarded as mutually closed: $M = (A|B)$. Each of them can in turn be represented by a collection of N_A and N_B mutually opened atoms, e.g., $A = (1_A : 2_A : \ldots : N_A)$. For that purpose, fragments' electron densities, $\rho_A(\boldsymbol{r})$ and $\rho_B(\boldsymbol{r})$, should be replaced with vectors grouping their atomic electron populations, or, more conveniently, partial atomic charges, $\boldsymbol{q}_A = \left(q_1^A, q_2^A, \ldots, q_{N_A}^A\right)$ and $\boldsymbol{q}_B = \left(q_1^B, q_2^B, \ldots, q_{N_B}^B\right)$. Similarly, fragments' external potentials, $v_A(\boldsymbol{r})$ and $v_B(\boldsymbol{r})$, are replaced with vectors $\boldsymbol{v}_A = \left(v_1^A, v_2^A, \ldots, v_{N_A}^A\right)$ and $\boldsymbol{v}_B = \left(v_1^B, v_2^B, \ldots, v_{N_B}^B\right)$. In such atomic resolution, the above-mentioned sensitivities can be represented as:

$$\mu_X = \left(\frac{\partial E}{\partial N_X}\right)_{N_Y, v_X, v_Y} \quad (4)$$

$$\eta_{X,Y} = \left(\frac{\partial^2 E}{\partial N_X \partial N_Y}\right)_{v_X, v_Y}, \qquad S_{X,Y} = \frac{1}{\eta_{X,Y}} \quad (5)$$

$$\boldsymbol{f}_{X,Y} = \left(-\frac{\partial \boldsymbol{q}_X}{\partial N_Y}\right)_{v_X, v_Y} = \left\{f_i^{X,Y} = \left(-\frac{\partial q_i^X}{\partial N_Y}\right)_{v_X, v_Y}\right\} \quad (6)$$

$$\boldsymbol{s}_{X,Y} = \left\{s_i^{X,Y} = f_i^{X,Y} S_{X,Y}\right\} \quad (7)$$

$$\boldsymbol{\beta}_{X,Y} = \left(-\frac{\partial \boldsymbol{q}_X}{\partial \boldsymbol{v}_Y}\right)_{N_X, N_Y} = \left\{\beta_{i,j}^{X,Y} = \left(-\frac{\partial q_i^X}{\partial v_j^Y}\right)_{N_X, N_Y}\right\} \quad (8)$$

where X and Y denote A or B.

As the reagents approach each other, charge transfer (CT) between them can be accounted for by coupling them to a common electron reservoir. The system then passes from a state of constrained equilibrium (different chemical potentials in A and B) to the state of global equilibrium with $\mu_A = \mu_B = \mu$.

Diagonal atomic Fukui indices, $f_i^{X,X}$, or alternatively atomic softnesses, $s_i^{X,X}$, can be used to probe inherent reactivities of different sites in the reagents. In the early works of Parr and Yang [47], it was suggested that sites with maximum values of Fukui function/local softness are the most reactive. This approach was later generalized by Li and Evans [61] by considering second-order electronic energy change accompanying reaction (3). According to the early works of Klopman [15] and Pearson [12], reactions between hard reagents are charge controlled (hard reactions) and reactions between soft reagents are orbital/charge transfer controlled (soft reactions). Li and Evans have shown that when CT is small, hard reactions proceed through atoms with minimal local softnesses, while soft reactions proceed through atoms of maximum local softness. These trends can be considered as the local counterpart of HSAB principle. When CT is large it can be shown [62] that regioselectivity is governed by Fukui indices and the character of the reagents. A reaction between neutral molecules proceeds through atoms with maximum Fukui indices. However, for reagents with large, usually opposite, total charges, the sites of minimum Fukui indices are preferred. This can be regarded as an intermediate hard/soft reaction when the CT is significant while the reagents are charged (i.e., hard). As indicated in Eqs. (2) and (7), Fukui indices and atomic softnesses are proportional to each other. Each of them can be used to probe relative atomic reactivities within one molecule. In the present study, atomic softnesses have been chosen because they also allow comparison between different molecules.

Computational details

In order to rule out any system-specific interactions, proton (H^+) was chosen as a model electrophilic agent. Geometrical structures of all possible tautomers of adenine and guanine in neutral, protonated and deprotonated states were optimized at DFT/B3LYP/6-31G* level of theory. Next, their energies were recalculated in the 6-31+G(3df,2p) basis. Solvent effects were modeled by performing analogous calculation with PCM model [63, 64] in a series of solvents with

dielectric constants (ε) varying from 1.88 (*n*-hexane) to 78.36 (water). All the calculations were performed with Gaussian09 program [65]. The most stable structures were chosen for CSA analysis. The calculations were performed with a program developed in our group. The details of the formalism are the same as in our previous studies [60, 66]. CSA results depend on the population analysis used to partition electron density into atomic contributions. For this reason, they were performed for six different analyses and their results have been compared. The analyses examined include the following: Mulliken population analysis (MPA) [67–69], natural population analysis (NPA) [70], Bader's atoms in molecules (AIM) [71, 72], Hirshfeld's stockholder analysis (HSA) [73], CHELPG electrostatic potential fitted charges [74, 75] and Voronoi deformation density (VDD)-based charges [76].

Results and discussion

One can think of two main mechanisms of proton's attack on purines. In the first (path **I**), proton attacks an anion and in the other (path **II**) a neutral molecule. In path **II**, the attack leads to a cationic transition state, which later undergoes deprotonation and the final neutral product is formed. In path **I**, the neutral product is formed directly by the attack of H$^+$ on the anion.

For adenine, 10 isomers of the neutral molecule (**A1–A10**), 5 anions (**AA1–AA5**) and 14 cations (**AC1–AC14**) have been considered. For guanine, 20 neutral molecules (**G1–G20**), 15 singly deprotonated anions (**GA1–GA15**) and 20 cations (**GC1–GC20**) have been analyzed. Guanine can also undergo double deprotonation. Experimental pK$_a$ value for this process equals to 12.3–12.4 [77–83]. Since such drastic conditions are rarely met in biological systems, this reaction path is not considered here. However, doubly deprotonated guanine anion (**GA16**) is used as a reference system in the discussion of CSA parameters and was included in the calculations. Optimized gas phase structures of all analyzed species, together with their energies, are gathered in Electronic Supplementary Materials available online (Figs. S1–S6). In what follows, isomers with energy within 10 kcal/mol from the most stable form, either in gas phase or in water, are considered. Their gas phase structures are presented in Figs. 1 and 2. The structures optimized in solutions were very similar to the gas phase ones and therefore are not presented.

Adenine

The energy diagram of adenine reactions with H$^+$ is presented in Fig. 3. The upper part of the diagram corresponds to reaction path **I**, the lower to path **II**. Above the dashes

Fig. 3 Energy diagram for reactions of adenine with H$^+$. The *first number* (*red*) above each *bar* represents the energy in the gas phase, the *second* (*blue*) in water (Color figure online)
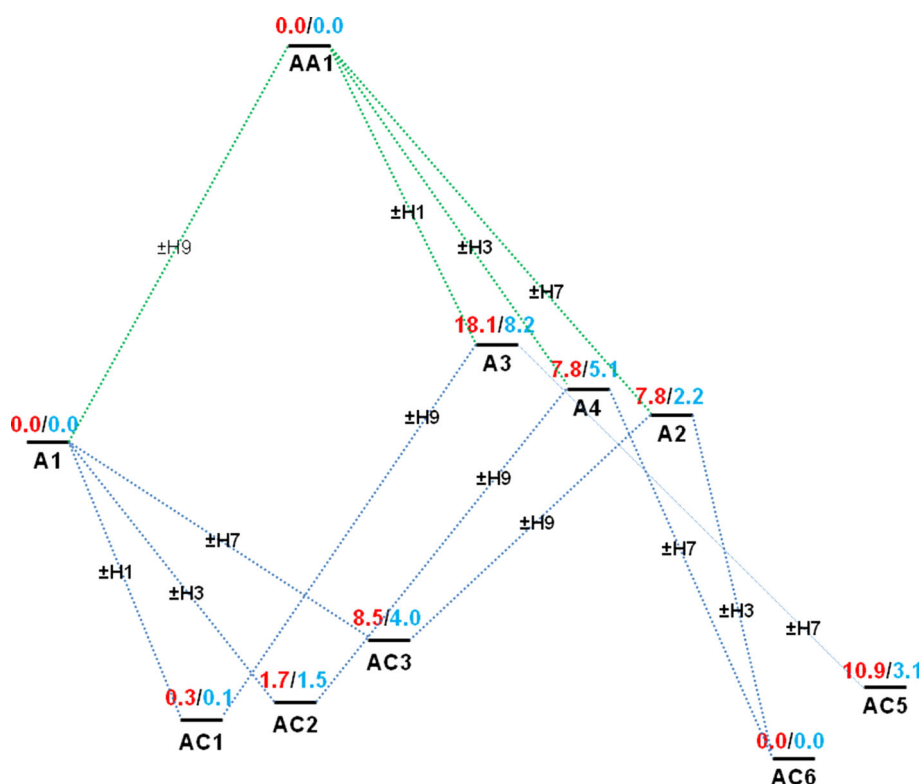
representing each structure are their energies calculated for two extreme environments: gas phase (red) and water (blue).

In the gas phase, neutral adenine can be found predominantly in the **A1** form, with proton at the *N9* position. Polarization by the solvent (Fig. 4a) does not change the energetic ordering of the lowest-energy isomers. It is manifested mainly by lowering the energy difference between **A1** and **A2** forms, up to 2.2 kcal/mol in water. Among adenine anions, the amine form **AA1** unequivocally dominates in the gas phase as well as in solutions. Therefore, reaction path **I** leads through electrophilic attack on **AA1**. Among neutral reaction products, *N9*-substituted **A1** isomer is the most favored. However, in polar solvents, some amounts of *N7*-substituted species can also be formed.

In the case of path **II**, in the gas phase it starts with H^+ attacking neutral molecule **A1**. Two low-energy cations can be produced in this process: **AC1**, **AC2**. Boltzmann distribution in 298 K leads to 91 and 9 % of **AC1** and **AC2**, respectively. Deprotonation of the transition products leads primarily to recreation of substrate **A1**. In polar solvents, the energies of **AC3**, **A2** and **A4** forms are lowered (Fig. 4 a, b). It allows **A2** and **A4** isomers to be created and undergo protonation to produce the lowest-energy cation, **AC6**. In these conditions, especially in protic solvents, one can assume that all the cations coexist as an equilibrium mixture. The contents of **AC6**, **AC1** and **AC2** then equal to 51, 45 and 4 %, respectively. Deprotonation of **AC6** leads to recreation of *N7*-substituted **A2** and possibly small amounts of *N3*-substituted **A4**. All in all, the most favored outcomes of the reaction are recreation of *N9*-substituted substrate and formation of the *N7*-substituted product. The latter is more probable in polar solvents.

In Fig. 5, partial atomic charges (top number) and atomic softnesses (bottom number, in braces) of nitrogen atoms are presented. They correspond to MPA population analysis. Results for other population analyses are presented in Supplementary Materials (Figs S7, S8).

In general, three types of nitrogen atoms can be distinguished in purines. The first one (N_I) involves exocyclic amine nitrogen with a mixed sp^2/sp^3 hybridization. In this sp^3 nitrogen atom, the lone electron pair is withdrawn by the aromatic system what introduces a partial sp^2 character. The second type (N_{II}) involves the nitrogen from the heterocyclic system with hydrogen attached. This sp^2 nitrogen has its lone pair delocalized in the aromatic system or involved in a bond with significant contribution of a double-bond character. The third group (N_{III}) contains heterocyclic sp^2 nitrogens without hydrogens. They donate a single electron to the heterocyclic system and therefore retain the lone pair.

In adenine, N_I atom is characterized by the largest, negative value of partial charge. This atom is in fact electron deficient. This deficiency is partially reduced by strong polarization of N–C and N–H bonds, which is responsible for large magnitude of its partial charge. The partial charges of N_{II} atoms are less negative. Finally, N_{III} atoms exhibit the least negative charges. Some small deviations from these trends can be observed in other population analyses. Nevertheless, in all population analyses, atomic softnesses exhibit a consistent trend. Electron-deficient character of N_I and N_{II} atoms is reflected by their low softness. Atoms belonging to these groups are not susceptible to electrophilic attack. N_{III} atoms possess lone electron pairs; thus, they exhibit the largest values of atomic softness. Atoms belonging to this group are the most susceptible to electrophilic attack.

To elucidate trends in relative reactivities of different sites in adenine, N_{III} atoms need to be compared. In **AA1** anion, purine's characteristic pattern of alternate N/C atoms is not perturbed by the presence of protons on the cyclic nitrogens. Moreover, partial charges and geometrical parameters (Figs. S1, S2 and S5) show that the negative charge is uniformly distributed in the heterocyclic system. Therefore, the trends observed for this species can be regarded as the most intrinsic for adenine. In this structure, nitrogen atoms from 6-membered ring are softer than these from the 5-membered ring. Moreover, $s_{N3} > s_{N1}$ and $s_{N9} > s_{N7}$. So the soft character of cyclic nitrogens increases in the series: $N7 < N9 < N1 < N3$. These trends are preserved in the neutral species.

On path **I**, reaction of **AA1** with H^+ proceeds between two oppositely charged species. According to Li–Evans model, it should proceed through atoms with low s_i values. These are the *N7* and *N9* atoms. s_{N7} is lower than s_{N9}—so from the purely kinetic point of view *N7* substitution is favored. This observation is in accordance with trends in energies of neutral adenine isomers. **A1** and **A2** forms result from attack on *N9* and *N7* and have low energies. Lower energy of **A1** is due to an unfavorable steric interaction between a proton from NH_2 group and *H7*, and not due to lower reactivity of *N7*. This is confirmed by significant lowering of the energy difference between **A1** and **A2** in water. **A3** and **A4** forms result from attack on soft *N3* and *N1* atoms. This path is less favored; hence, **A3** and **A4** have larger energies. The energy of **A4** is less decreased in water than that of **A2**. This confirms that the destabilization of **A4** comes mainly from electronic effects. In the case of **A3**, both destabilizing factors, electronic and steric, cooperate. These results are in agreement with experimental observations, i.e., in basic conditions the reaction with a variety of reagents proceeds on *N9* [20, 24, 84, 85].

In reactions on path **II**, a cation attacks a neutral molecule. Again, the atom with minimum softness, i.e., *N7*, is the favorable site of attack. Different preferences can be expected according to relative energies of the cations. As
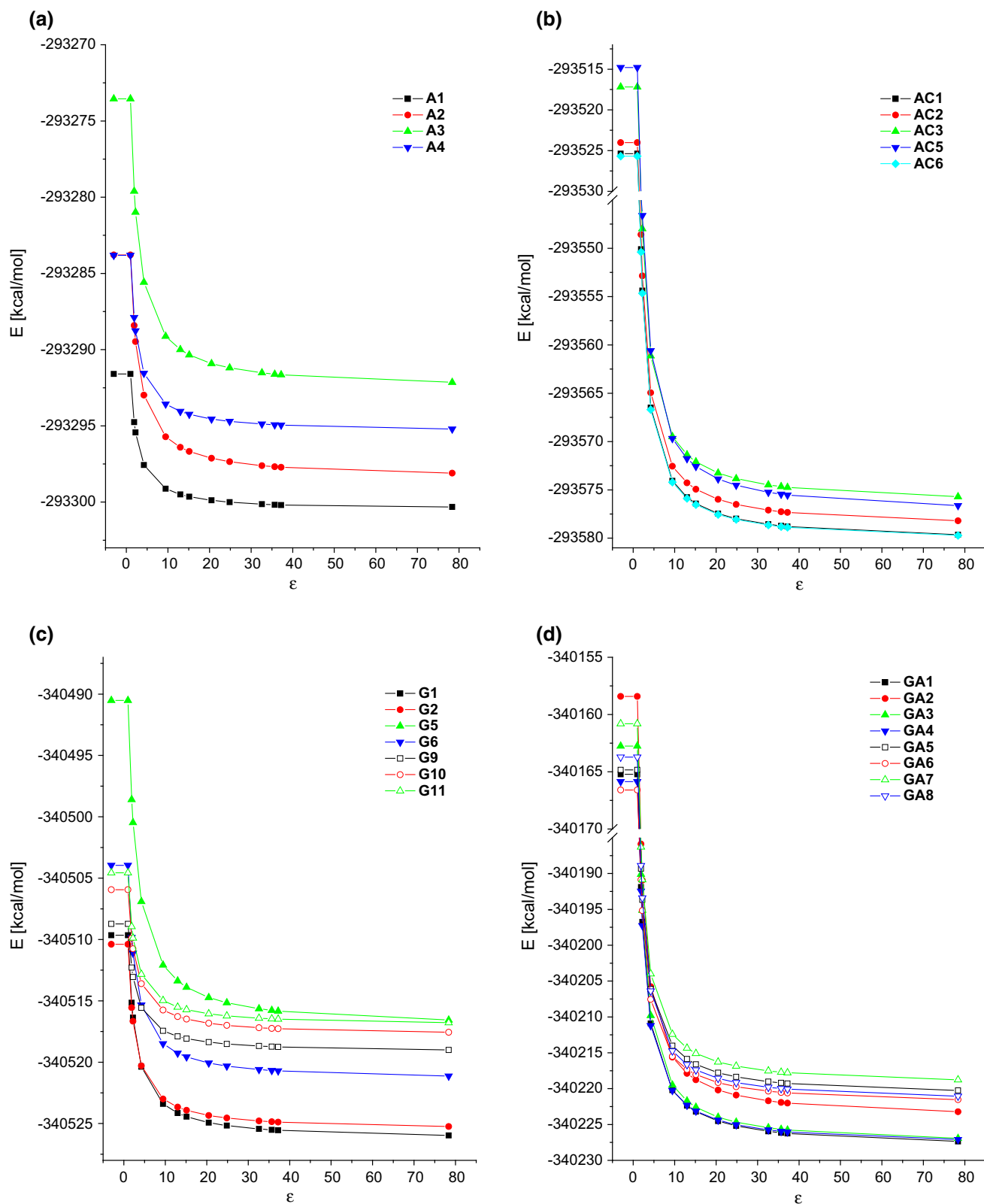
Fig. 4 Influence of solvents with different dielectric constants on the energies of neutral (**a**) and protonated (**b**) adenine, neutral guanine (**c**) isomers and guanine anions (**d**). Energetic order of the isomers in the gas phase is depicted as *horizontal lines* in the range of negative ε
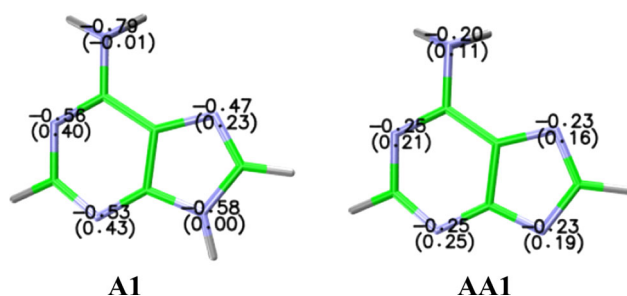
**Fig. 5** Partial atomic charges (MPA) and atomic softnesses of nitrogen atoms in adenine and its anion

stated above, the stability of cations decreases in the series: **AC1** > **AC2** > **AC3**, so *N1* site is preferred over *N3* and *N7*, with the latter being strongly disfavored. These discrepancies are caused by the large change in external potential introduced by the attacking H⁺. In adenine cations, electron delocalization determines their relative energies. The lone electron pair of *N6* atom is conjugated with the heterocyclic ring, and the whole system is flat. The presence of a hydrogen atom in *N1* position allows for advantageous electron delocalization over both heterocyclic rings. This is not possible in *N7*- and *N3*-substituted products. Additional destabilization of the former is introduced by the steric interaction between *H7* and *H6* atoms. *N7* substitution is therefore favored in terms of inherent reactivity of isolated substrate, while *N1* substitution is favored energetically. Experimental results show that

reactivity criteria dominate and that *N7*-substituted products are observed in neutral pH [3, 86].

Guanine

In the case of guanine, manifold of possible tautomeric forms makes the picture somewhat more complex. The energy diagram of its reactions with H⁺ (Fig. 6) shows that in the gas phase it exists as a mixture of two main isomers: **G1** and **G2**. Both of them have a proton in *N1* position. They differ in the position of the second proton (*N9* in **G1** and *N7* in **G2**). Small amounts of enolamine form **G9** can also be found. In 298 K, Boltzmann distribution leads to 21, 74 and 5 % of isomers **G1**, **G2** and **G9**, respectively. In solutions, the ordering of **G1** and **G2** forms interchanges as ε rises (Fig. 4c). At the same time, the energy of **G9** isomer rises relative to **G1**, up to 7 kcal/mol in water. In this solvent, the amounts of guanine isomers equal to 77 and 23 % of **G1** and **G2**, respectively. These results are in qualitative agreement with a more accurate study of Goddard and co-workers who report 32 % of **G1** in the gas phase and 88 % in water [30]. As already pointed out by Goddard, these differences in relative energies are due to two factors. Firstly, **G1** has a larger dipole moment than **G2**, and therefore, its solvation energy is greater. Secondly, in **G1** and **G2** forms unfavorable steric interactions between the protons from NH₂ group and *N1* position are shielded in polar solvents. This causes their energies to be lowered with respect to **G9** isomer.

Fig. 6 Energy diagram for reactions of guanine with H⁺. The *first number* (*red*) above each *bar* represents the energy in the gas phase, the *second* (*blue*) in water (Color figure online)
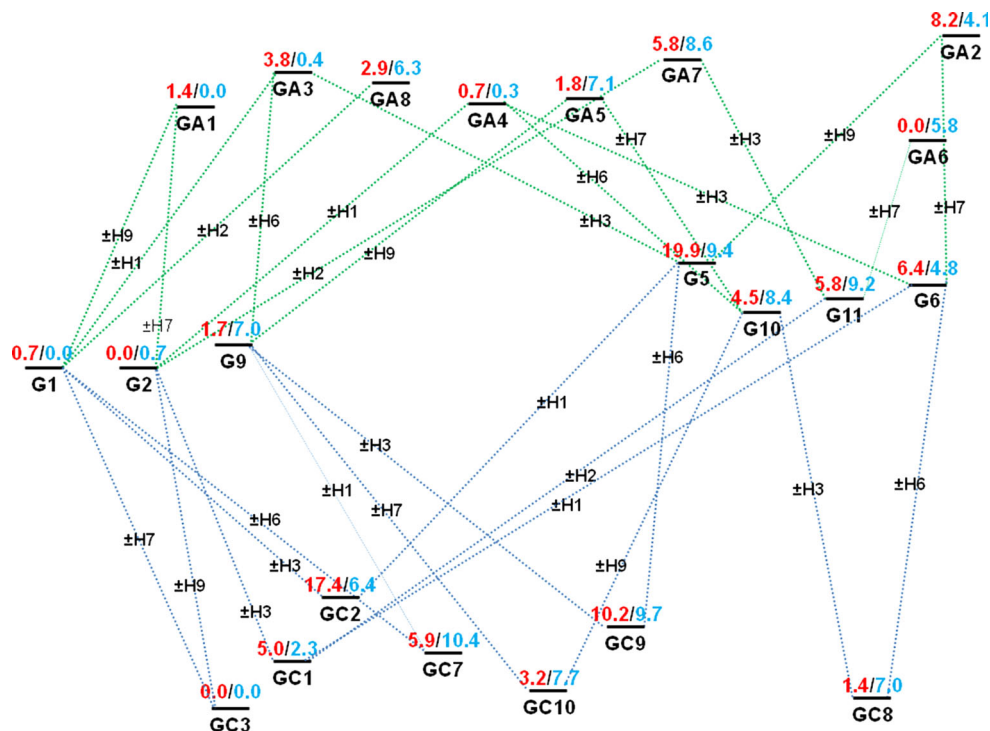
In the gas phase, single deprotonation of isomers **G1**, **G2** and **G9** leads to three low-energy anions: **GA1**, **GA4** and **GA5**. After accounting for the relative contents of neutral species, their amounts equal to 38, 55 and 4 %, respectively. However, similar to the case of adenine cations, the most stable anion, **GA6**, is not produced by direct deprotonation of any of the low-energy neutral species. This picture changes in solutions (Fig. 4d). As the dielectric constants of the solvent rises, the energies of **GA5** and **GA6** quickly rise. At the same time, the energies of **GA1** and **GA3** are lowered with respect to **GA4**. In water, the amounts of **GA1**, **GA3** and **GA4** are equal to 47, 23 and 30 %, respectively. Again, these trends can be rationalized in terms of dipole moment differences and shielding unfavorable steric interactions.

To sum up, in the gas phase, reactions on path **I** proceed through anions **GA1**, **GA4** and **GA5**. Attack on **GA1** leads to a mixture of products substituted at positions *N9* and *N7* (**G1** and **G2**). Attack on **GA4** produces mainly **G2** form. Attack on **GA5** leads to enolamine isomer **G9**. In water, the reaction may proceed through **GA1**, **GA3** or **GA4** anions. Again, attack on **GA1** leads to a mixture of **G1** and **G2** products. **G1** is also produced by attack on **GA3**, while **G2** is produced by attack on **GA4**. Therefore, all in all *N7*- and *N9*-substituted products are favored.

In the case of guanine cations, one low-energy structure, i.e., **GC3**, dominates in the gas phase. It is produced directly from protonation of either **G1** or **G2**. Formation of the other low-energy cation, **GC8**, is unlikely due to high energies of its antecedents, **G10** and **G6**. In solutions, the energy of **GC8** quickly increases. At the same time, the energy difference between **GC3** and **GC1** decreases, up to 2 kcal/mol in water. Deprotonation of **GC3** leads back to **G1** and **G2** neutral systems Therefore, in the gas phase reactions on path **II** lead to a mixture of *N7*- and *N9*-substituted products. This is not changed in solutions since formation of **GC1** cation leads primarily to recreation of the substrate, **G2**.

Figure 7 presents partial charges and atomic softnesses of nitrogen and oxygen atoms in guanine and its ions. Again, the same three types of N atoms can be distinguished. Their main characteristics remain unchanged. Additional type of nitrogen (N_{IV}), i.e., *N2* imine nitrogen, can be found in **G9** and **GA5** systems. It forms a double bond with C2 and retains the lone pair. It is characterized by low, negative partial charge and large softness. It is susceptible to electrophilic attack. Two types of oxygen atoms can be distinguished: carbonyl (O_I) and hydroxyl (O_{II}). Carbonyl oxygens exhibit a partial charge comparable to those of N_{III} nitrogens. The softness of O_I atoms unequivocally dominates among other atomic softnesses in the system. In analogy to N atoms, magnitude of oxygen's partial charge increases upon protonation, while its softness drops.

Doubly deprotonated anion, **GA16,** can serve as a model of guanine's heterocyclic system, unperturbed by the presence of hydrogens. From data in Fig. 7, it can be seen that in this species negative charge is distributed among all the electronegative atoms. Geometrical parameters (Fig. S4) suggest that in contrast to adenine anion **AA1**, in **GA16** the presence of a carbonyl group disables the heterocyclic rings from attaining a fully aromatic character. Nevertheless, partial charges and atomic softnesses of N_{III} atoms exhibit similar trends to **AA1**. The only exception is that nitrogens from 5- and 6-membered rings have in pairs similar softness values. Thus, nucleophilic character of N_{III} atoms increases in the series: $N7 \approx N9 < N1 \approx N3$. It can also be seen that the lone pair of *N2* atom is no longer withdrawn by the heterocyclic system. It is reflected in the value of its atomic softness, which is in the same range as those of N_{III} atoms. Therefore, sp^3 nitrogens which retain their lone pairs are also susceptible to electrophilic attack. Also electron-rich carbonyl oxygen has a large value of atomic softness.

When an N_{III} atom in **GA16** is protonated, its atomic softness and partial charge change in the same way as previously described for adenine. Interestingly, protonation of *N1* atom causes also a decrease in the softness of *N3* atom. On the contrary, in 5-membered ring protonation of one of the nitrogens makes the other softer. Protonation of *O6* decreases softnesses of all N_{III} atoms, especially *N7*. In singly deprotonated anions, protonation of nitrogen atoms preserves the observed trends. Upon protonation of *O6* s_{N1} now decreases the most. These trends rationalize the observed softness values in neutral species. In **G1** and **G2** systems, the increase in s_{N7} or s_{N9} and decrease in s_{N3} are responsible for the greater values of N_{III} atoms' softnesses in 5-membered ring than those of nitrogens in 6-membered ring. Similarly, lower value of s_{N1} than s_{N3} in **G9** can be attributed to the protonation of *O6*.

As previously stated, sites with minimum softness values are preferred for the attack on both reaction paths. In pH between 9.4 and 12.5, depending on the polarity of the solvent three singly deprotonated anions, **GA1**, **GA3** and **GA4**, can be present. In all of these structures, softnesses of all N_{III} atoms are close to each other. Some subtle trends that can be observed are not equivocal and depend on the population analysis. Therefore, kinetic control does not favor any of the products definitely. In this case, the observed products should depend on thermodynamic control. Depending on the polarity of the solvent, those can be *N7*-, *N9*- or *N1*-substituted species. Accounting for the fact that both the anions and the products of their protonation exist as mixtures of different isomers, all three N-substituted species can be expected. Therefore, neither reactivity nor energetic parameters do unequivocally favor a specific site of the reaction. When H^+ is attacking a neutral guanine
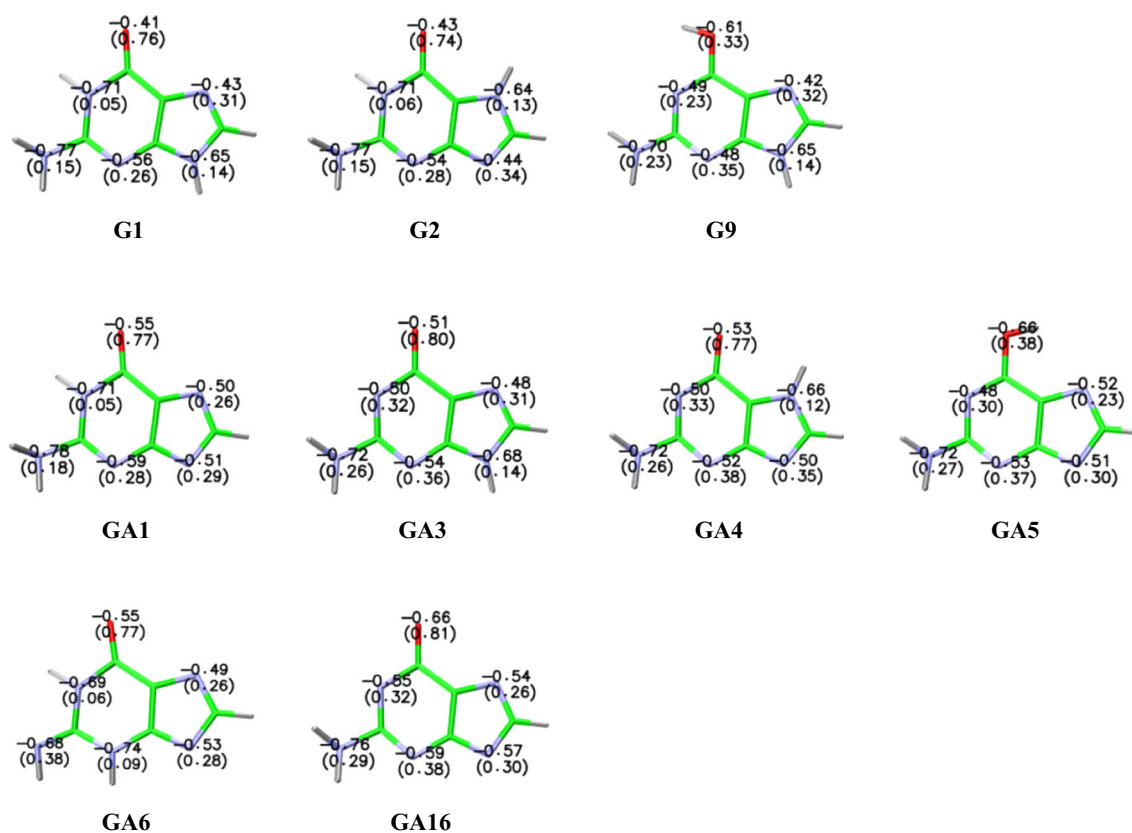
Fig. 7 Partial atomic charges (MPA) and atomic softnesses of nitrogen and oxygen atoms in guanine and its anions

molecule (pH < 9), *N3* site is the most reactive. Yet, attack on this atom is strongly disfavored energetically. This explains the lack of adducts observed experimentally in these conditions [3].

The results gathered in Supplementary Materials show that with some minor exceptions NPA, HSA and VDD analyses predict similar trends to MPA. AIM analysis on the other hand clearly stands out of the others, giving results which are often in contradiction with all the remaining analyses. For this reason, it should probably be discouraged in similar studies. CHELPG analysis sometimes agrees with the others and sometimes it does not. What is more, it often produces negative values of atomic softnesses, which are somewhat questionable [87]. They are most probably due to the statistical inaccuracy introduced by the charge-fitting procedure. Therefore, its use may also be disfavored. MPA and NPA analyses as well as HSA and VDD give in pairs very similar results. This is not surprising since they are based on similar theoretical backgrounds. The results of MPA and NPA pair are probably closest to conventional chemical intuition regarding magnitude of the atomic charges and softnesses. A better agreement with experimental data has also been observed for these analyses, with MPA being slightly superior. In conclusion, these two schemes can be advised as most reliable in similar studies.

The choice of NPA or HSA analyses has in fact already been suggested by others [87].

Conclusions and future prospects

In the presented study, DFT calculations have been employed to model nucleophilic reactivity of purine bases. The energetics of their protonation/deprotonation in different media have been examined with the PCM model. CSA calculations have been used to study charge distribution and relative reactivity of different sites. It is shown that this approach is very successful in predicting regioselectivity of electrophilic attack on these ambidente species. It enables separation of two different contributions, i.e., inherent reactivity and the influence of reaction conditions, to regioselectivity. This in turn allows elucidating and rationalizing clear trends in the otherwise perplexing manifold of experimental data. The results obtained in the present study are in agreement with experimentally observed products of reactions with various electrophiles and in various conditions.

In empirical organic chemistry, Kornblum's rule is often used to rationalize observed regioselectivity of electrophilic attack on ambidente nucleophiles. It originally

stated that hard electrophiles react with the most electronegative sites in the nucleophile, while soft electrophiles tend to attack less electronegative, soft atoms. It was later combined with empirical HSAB principle. Recently, this approach has been criticized by Mayr et al. [88]. They argue that the number of cases where empirical HSAB approach fails is almost equal to that of its successes. In the discussed case of electrophilic attack on purines, Kornblum's rule also fails. For guanine, it predicts that hard electrophiles should attack the oxygen atom. The present study shows that despite large electronegativity of $O6$, this atom is actually very soft. Therefore, extremely hard H^+ attacks nitrogen atoms. Indeed, O-substituted products are rarely observed experimentally and often in small yields. It seems that their formation is due to some specific interactions between the reagents or other species present in the reaction mixture. Similar situation was observed for alkylation of 2-pyridone on the basis of which Kornblum formulated his rule [89, 90]. The present study demonstrates that, despite the failure of Kornblum's rule, the concept of HSAB itself does not need to be discarded. The main deficiency of empirical HSAB is the inaccurate definition of hardness/softness. Thanks to development introduced in this field by conceptual DFT; this problem can be solved. This, as well as many other successful theoretical studies [34] show that the concept of HSAB is in fact justified and very useful.

As far as biological consequences are concerned another issue needs to be addressed, i.e., the influence of the chemical neighborhood of the nucleobases on their reactivity. For example, Fishbein and co-workers have demonstrated that the highest nucleophilic activity of $N1$ atom of adenine is actually due to the structure of the DNA helix and not to inherent properties of this nucleobase [91]. One aspect of this problem is the geometrical availability of particular sites in the DNA helix. Another is the electrostatic environment of individual atoms and its influence of on their reactivity. We have recently demonstrated that atomic Fukui indices as well as other charge sensitivities change when an atom is engaged in a hydrogen bond [60]. Also the bond with the sugar moiety can influence the electronic properties of the heterocyclic ring. Studies in this direction are carried out in our group.

Extremely low computational cost of CSA scheme makes it especially well suited for studies of large systems. It can further be combined with molecular dynamics calculations in order to include many-body effects in the simulations. Similar electronegativity-based approaches are already known in the literature under the name of fluctuating charge models [92–96]. However, CSA offers a much broader perspective. As evidenced above, it provides reliable information about the reactivity of particular sites in the system. In this respect, the agreement of CSA reactivity parameters with experimental results, and also with commonly recognized chemical intuition, is especially encouraging. Our previous study [60] also indicates that various charge sensitivities can be used as bond detectors. All these features of CSA can be utilized in construction of a reactive force field. We have undertaken steps in this direction.

References

1. Enoch SJ, Cronin MTD (2010) A review of the electrophilic reaction chemistry involved in covalent DNA binding. Crit Rev Toxicol 40:728–748. doi:10.3109/10408444.2010.494175
2. Stone MP, Huang H, Brown KL, Shanmugam G (2011) Chemistry and structural biology of DNA damage and biological consequences. Chem Biodivers 8:1571–1615. doi:10.1002/cbdv.201100033
3. Xue W, Siner A, Rance M et al (2002) A metabolic activation mechanism of 7H-dibenzo[c, g]carbazole via o-quinone. Part 2: covalent adducts of 7H-dibenzo[c, g]carbazole-3,4-dione with nucleic acid bases and nucleosides. Chem Res Toxicol 15:915–921
4. Eder E, Hoffman C, Bastian H et al (1990) Molecular mechanisms of DNA damage initiated by alpha, beta-unsaturated carbonyl compounds as criteria for genotoxicity and mutagenicity. Environ Health Perspect 88:99–106
5. Bolton JL, Pisha E, Zhang F, Qiu S (1998) Role of quinoids in estrogen carcinogenesis. Chem Res Toxicol 11:1113–1127. doi:10.1021/tx9801007
6. Bolton JL, Thatcher GRJ (2008) Potential mechanisms of estrogen quinone carcinogenesis. Chem Res Toxicol 21:1113–1127. doi:10.1021/tx700191p
7. Wang H, Kozekov ID, Harris TM, Rizzo CJ (2003) Site-specific synthesis and reactivity of oligonucleotides containing stereochemically defined 1, N2-deoxyguanosine adducts of the lipid peroxidation product trans-4-hydroxynonenal. J Am Chem Soc 125:5687–5700. doi:10.1021/ja0288800
8. Stone MP, Cho Y, Huang HAI et al (2008) Interstrand DNA cross-links induced by a, b-unsaturated aldehydes derived from lipid peroxidation and environmental sources. Acc Chem Res 41:793–804
9. Woo J, Snorri TS, Hopkins PB (1993) DNA interstrand cross-linking reactions of pyrrole-derived, bifunctional electrophiles: evidence for a common target site in DNA. J Am Chem Soc 115:3407–3415
10. Boysen G, Pachkowski BF, Nakamura J, Swenberg JA (2009) The formation and biological significance of N7-guanine adducts. Mutat Res 678:76–94. doi:10.1016/j.mrgentox.2009.05.006
11. Berson JA (2006) Kinetics, thermodynamics, and the problem of selectivity: the maturation of an idea. Angew Chem Int Ed 45:4724–4729. doi:10.1002/anie.200600229
12. Pearson RG (1963) Hard and soft acids and bases. J Am Chem Soc 85:3533–3539

13. Pearson RG, Songstad J (1966) Application of the principle of hard and soft acids and bases to organic chemistry. J Am Chem Soc 89:1827–1836

14. Kornblum N, Smiley RA, Blackwood RK, Iffland DC (1955) The mechanism of the reaction of silver nitrite with alkyl halides. The contrasting reactions of silver and alkali metal salts with alkyl halides. The alkylation of ambient anions. J Am Chem Soc 77:6269–6280

15. Klopman G (1968) Chemical reactivity and the concept of charge-and-frontier controlled reactions. J Am Chem Soc 90:223–234

16. Royer RE, Lyle TA, Moy GG et al (1979) Reactivity-selectivity properties of reactions of carcinogenic electrophiles with biomolecules. Kinetics and product of the reaction of benzo[a]-6-methyl cation with nucleosides and deoxynucleosides. J Org Chem 44:3202–3207

17. Moschel RC, Hudgins WR, Dipple A (1979) Selectivity in nucleoside alkylation and aralkylation in relation to chemical carcinogenesis. J Org Chem 44:3324–3328. doi:10.1021/jo01333a010

18. Wang H, Meng F (2010) Theoretical study of proton-catalyzed hydrolytic deamination mechanism of adenine. Theor Chem Acc 127:561–571. doi:10.1007/s00214-010-0747-1

19. Freccero M, Gandolfi R, Sarzi-Amadè M (2003) Selectivity of purine alkylation by a quinone methide. Kinetic or thermodynamic control? J Org Chem 68:6411–6423. doi:10.1021/jo0346252

20. Holy A, Gunter J, Dvorakova H et al (1999) Structure-antiviral activity relationship in the series of pyrimidine and purine N-[2-(2-(phosphonomethoxy)ethyl] nucleoside analogues. 1. Derivatives substituted at the carbon atoms of the base. J Med Chem 42:2064–2086

21. Veldhuyzen WF, Lam YF, Rokita SE (2001) 2′-Deoxyguanosine reacts with a model quinone methide at multiple sites. Chem Res Toxicol 14:1345–1351

22. Weinert EE, Frankenfield KN, Rokita SE (2005) Time-dependent evolution of adducts formed between deoxynucleosides and a model quinone methide. Chem Res Toxicol 18:1364–1370. doi:10.1021/tx0501583

23. Pawłowicz AJ, Munter T, Zhao Y, Kronberg L (2006) Formation of acrolein adducts with 2′-deoxyadenosine in calf thymus DNA. Chem Res Toxicol 19:571–576. doi:10.1021/tx0503496

24. Breugst M, Corral Bautista F, Mayr H (2012) Nucleophilic reactivities of the anions of nucleobases and their subunits. Chem A Eur J 18:127–137. doi:10.1002/chem.201102411

25. Lee HM, Chae Y-H, Kwon C, Kim SK (2007) Conformations of adducts formed between the genotoxic benzo[a]pyrene-7,8-dione and nucleosides studied by density functional theory. Biophys Chem 125:151–158. doi:10.1016/j.bpc.2006.07.015

26. Ford GP, Scribner JD (1990) Prediction of nucleoside-carcinogen reactivity. Alkylation of adenine, cytosine, guanine, and thymine and their deoxynucleosides by alkanediazonium ions. Chem Res Toxicol 3:219–230

27. Parr RG, Yang W (1989) Density functional theory of atoms and molecules. Oxford University Press, Oxford

28. Bren U, Guengerich FP, Mavri J (2007) Guanine alkylation by the potent carcinogen aflatoxin B1: quantum chemical calculations. Chem Res Toxicol 20:1134–1140. doi:10.1021/tx700073d

29. Bren U, Zupan M, Guengerich FP, Mavri J (2006) Chemical reactivity as a tool to study carcinogenicity: reaction between chloroethylene oxide and guanine. J Org Chem 71:4078–4084. doi:10.1021/jo060098l

30. Jang YH, Goddard WA III, Noyes KT et al (2003) pK a values of guanine in water : density functional theory calculations combined with Poisson-Boltzmann continuum-solvation model. J Phys Chem B 107:344–357

31. Shukla PK, Ganapathy V, Mishra PC (2011) A quantum theoretical study of reactions of methyldiazonium ion with DNA base pairs. Chem Phys 388:31–37. doi:10.1016/j.chemphys.2011.07.014

32. Xing D, Sun L, Cukier RI, Bu Y (2007) Theoretical prediction of the p53 gene mutagenic mechanism induced by trans-4-hydroxy-2-nonenal. J Phys Chem B 111:5362–5371

33. Geerlings P, De Proft F, Langenaeker W (2003) Conceptual density functional theory. Chem Rev 103:1793–1873. doi:10.1021/cr990029p

34. Chattaraj PK (2009) Chemical reactivity theory: a density functional view. CRC Press, Boca Raton

35. Yang W, Parr RG (1985) Hardness, softness, and the Fukui function in the electronic theory of metals and catalysis. Proc Natl Acad Sci U S A 82:6723–6726

36. Parr RG, Szentpaly L, Liu S (1999) Electrophilicity index. J Am Chem Soc 121:1922–1924. doi:10.1021/ja983494x

37. Chattaraj PK, Sarkar U, Roy DR (2006) Electrophilicity index. Chem Rev 106:2065–2091. doi:10.1021/cr040109f

38. Jaramillo P, Pérez P, Contreras R et al (2006) Definition of a nucleophilicity scale. J Phys Chem A 110:8181–8187. doi:10.1021/jp057351q

39. Anderson JSM, Melin J, Ayers PW (2007) Conceptual density-functional theory for general chemical reactions, including those that are neither charge- nor orbital-controlled. 2. Application to molecules where frontier molecular orbital theory fails. J Chem Theory Comput 3:375–389

40. LoPachin RM, Gavin T, Decaprio A, Barber DS (2012) Application of the hard and soft, acids and bases (HSAB) theory to toxicant–target interactions. Chem Res Toxicol 25:239–251. doi:10.1021/tx2003257

41. Nalewajski RF, Korchowiec J (1998) Charge sensitivity approach to electronic structure and chemical reactivity. World Scientific Publishing, Singapore

42. Stachowicz A, Styrcz A, Korchowiec J (2011) Charge sensitivity analysis in force-field-atom resolution. J Mol Model 17:2217–2226. doi:10.1007/s00894-011-1006-7

43. Stachowicz A, Korchowiec J (2012) Generalized charge sensitivity analysis. J Struct Chem 23:1449–1458

44. Donnelly RA, Parr RG (1978) Elementary properties of an energy functional of the first-order reduced density matrix. J Chem Phys 69:4431. doi:10.1063/1.436433

45. Parr RG, Pearson RG (1983) Absolute hardness: companion parameter to absolute electronegativity. J Am Chem Soc 105:7512–7516. doi:10.1021/ja00364a005

46. Berkowitz M, Parr RG (1988) Molecular hardness and softness, local hardness and softness, hardness and softness kernels, and relations among these quantities. J Chem Phys 88:2554. doi:10.1063/1.454034

47. Parr RG, Yang W (1984) Density functional approach to the frontier-electron theory of chemical reactivity. J Am Chem Soc 106:4049–4050

48. Politzer P, Weinstein H (1979) Some relations between electronic distribution and electronegativity. J Chem Phys 71:4218. doi:10.1063/1.438228

49. Sanderson RT (1951) An interpretation of bond lengths and a classification of bonds. Science 114:670–672. doi:10.2307/1678148

50. Sanderson RT (1976) Chemical bonds and bond energy. Academic Press, New York

51. Ghanty TK, Ghosh SK (1993) Correlation between hardness, polarizability, and size of atoms, molecules, and clusters. J Chem Phys 97:4951–4953

52. Ayers PW (2007) The physical basis of the hard/soft acid/base principle. Faraday Discuss 135:161. doi:10.1039/b606877d

53. Chattaraj PK, Lee H, Parr RG (1991) HSAB principle. J Am Chem Soc 113:1855–1856

54. Ayers PW (2005) An elementary derivation of the hard/soft-acid/base principle. J Chem Phys 122:141102. doi:10.1063/1.1897374

55. Ayers PW, Parr RG, Pearson RG (2006) Elucidating the hard/soft acid/base principle: a perspective based on half-reactions. J Chem Phys 124:194107. doi:10.1063/1.2196882

56. Sablon N, De Proft F, Geerlings P (2010) The linear response kernel of conceptual DFT as a measure of electron delocalisation. Chem Phys Lett 498:192–197. doi:10.1016/j.cplett.2010.08.031

57. Sablon N, De Proft F, Solà M, Geerlings P (2012) The linear response kernel of conceptual DFT as a measure of aromaticity. Phys Chem Chem Phys 14:3960–3967. doi:10.1039/c2cp23372j

58. Fias S, Boisdenghien Z, Stuyver T et al (2013) Analysis of aromaticity in planar metal systems using the linear response kernel. J Phys Chem A 117:3556–3560. doi:10.1021/jp401760j

59. Fias S, Geerlings P, Ayers P, De Proft F (2013) Σ, Π aromaticity and anti-aromaticity as retrieved by the linear response kernel. Phys Chem Chem Phys 15:2882–2889. doi:10.1039/c2cp43612d

60. Stachowicz A, Korchowiec J (2013) Bond detectors for molecular dynamics simulations, part I: hydrogen bonds. J Comput Chem 34:2261–2269. doi:10.1002/jcc.23385

61. Li Y, Evans JNS (1995) The Fukui function: a key concept linking frontier molecular orbital theory and the hard-soft-acid-base principle. J Am Chem Soc 117:7756–7759. doi:10.1021/ja00134a021

62. Berkowitz M, Ghosh SK, Parr RG (1985) On the concept of local hardness in chemistry. J Am Chem Soc 107:6811–6814. doi:10.1021/ja00310a011

63. Cossi M, Scalmani G, Rega N, Barone V (2002) New developments in the polarizable continuum model for quantum mechanical and classical calculations on molecules in solution. J Chem Phys 117:43. doi:10.1063/1.1480445

64. Cossi M, Rega N, Scalmani G, Barone V (2001) Polarizable dielectric model of solvation with inclusion of charge penetration effects. J Chem Phys 114:5691. doi:10.1063/1.1354187

65. Frisch MJ, Trucks GW, Schlegel HB, Scuseria GE, Robb MA, Cheeseman JR, Scalmani G, Barone V, Mennucci B, Petersson GA, Nakatsuji H, Caricato M, Li X, Hratchian HP, Izmaylov AF, Bloino J, Zheng G, Sonnenberg JL, Hada M, Ehara M, Toyota K, Fukuda R, Hasegawa J, Ishida M, Nakajima T, Honda Y, Kitao O, Nakai H, Vreven T, Montgomery JA, Peralta JE Jr, Ogliaro F, Bearpark M, Heyd JJ, Brothers E, Kudin KN, Staroverov VN, Kobayashi R, Normand J, Raghavachari K, Rendell A, Burant JC, Iyengar SS, Tomasi J, Cossi M, Rega N, Millam JM, Klene M, Knox JE, Cross JB, Bakken V, Adamo C, Jaramillo J, Gomperts R, Stratmann RE, Yazyev O, Austin AJ, Cammi R, Pomelli C, Ochterski JW, Martin RL, Morokuma K, Zakrzewski VG, Voth GA, Salvador P, Dannenberg JJ, Dapprich S, Daniels AD, Farkas Ö, Foresman JB, Ortiz JV, Cioslowski J, Fox DJ (2013) Gaussian 09, Revision D.01. Gaussian Inc., Wallingford CT

66. Stachowicz A, Rogalski M, Korchowiec J (2013) Charge sensitivity approach to mutual polarization of reactants: molecular mechanics perspective. J Mol Model. doi:10.1007/s00894-013-1757-4

67. Mulliken RS (1955) Electronic population analysis on LCAO–MO molecular wave functions. I. J Chem Phys 23:1833–1840

68. Mulliken RS (1955) Electronic population on LCAO–MO molecular wave functions. II. Overlap populations, bond orders, abd covalent bond energies. J Chem Phys 23:1841–1846

69. Mulliken RS (1955) Electronic population analysis on LCAO–MO molecular wave functions. III. Effects of hybridization on overlap and gross AO populations. J Chem Phys 23:2338–2342

70. Reed AE, Weinstock RB, Weinhold F (1985) Natural population analysis. J Chem Phys 83:735. doi:10.1063/1.449486

71. Bader RFW (1990) Atoms-in-molecules. Oxford University Press, Oxford

72. Bader RFW (1991) A quantum theory of molecular structure and its applications. Chem Rev 91:893–928

73. Hirshfeld FL (1977) Bonded-atom fragments for describing molecular charge densities. Theor Chim Acta 44:129–138. doi:10.1007/BF00549096

74. Chirlian LE, Francl MM (1987) Atomic charges derived from electrostatic potentials: a detailed study. J Comput Chem 8:894–905. doi:10.1002/jcc.540080616

75. Breneman CM, Wiberg KB (1990) Determining atom-centered monopoles from molecular electrostatic potentials. The need for high sampling density in formamide conformational analysis. J Comput Chem 11:361–373. doi:10.1002/jcc.540110311

76. Bickelhaupt FM, van Eikema Hommes NJR, Guerra FC, Baerends EJ (1996) The carbon–lithium electron pair bond in $(CH_3Li)n$ (n = 1, 2, 4). Org Lett 15:2923–2931

77. Bundari S (1996) The Merck Index, 12th edn. Merck and Co., Inc., Whitehouse Station

78. Chargaff E, Davidson JN (1955) The nucleic acids. Chemistry and biology. Academic Press Inc., New York

79. Haynes WM (2012) CRC handbook of chemistry and physics, 93rd edn. CRC Press, Taylor & Francis Group, Boca Raton

80. Dawson RMC, Elliott DC, Elliott WH, Jones KM (1986) Data for biochemical research, 3rd edn. Oxford University Press, Oxford

81. Fasman GD (1975) CRC handbook of biochemistry and molecular biology. nucleic acids, 3rd edn. CRC Press, Taylor & Francis Group, Cleaveland

82. Jordan DO (1960) The chemistry of nucleic acids. Butterworth and Co., Washington

83. Ts'o POP (1974) Basic principles in nucleic acid chemistry. Academic Press, New York

84. Taddei M, Ciapetti P (1998) A simple preparation of N-vinyl derivatives of DNA nucleobases. Tetrahedron 54:11305

85. Browne DT, Eisinger J, Leonard NJ (1968) Synthetic spectroscopic models related to coenzymes and base pairs. II. Evidence for intramolecular base–base interactions in dinucleotide analog. J Am Chem Soc 90:7302–7323

86. Reiner B, Zamenhof S (1957) Studies on the chemically reactive groups of deoxyribonucleic acids. J Biol Chem 228:475–486

87. Kinkar Roy R, Hirao K, Pal S (2000) On non-negativity of Fukui function indices. II. J Chem Phys 113:1372. doi:10.1063/1.481927

88. Mayr H, Breugst M, Ofial AR (2011) Farewell to the HSAB treatment of ambident reactivity. Angew Chem Int Ed Engl 50:6470–6505. doi:10.1002/anie.201007100

89. Anderson DR, Keute JS, Koch TH, Moseley RH (1977) Di-tert-butyl nitroxide quenching of the photoaddition of olefins to the carbon–nitrogen double bond of 3-ethoxyisoindolenone. J Am Chem Soc 99:6332–6340

90. Tao X, Li Y-Q, Xu H-H et al (2009) Synthesis and characterization of organophosphine/phosphite stabilized N-silver(I) succinimide: crystal structure of [(Ph3P)3·AgNC4H4O2]. Polyhedron 28:1191–1195. doi:10.1016/j.poly.2009.02.021

91. Lu X, Heilman JM, Blans P, Fishbein JC (2005) The structure of DNA dictates purine atom site selectivity in alkylation by primary diazonium ions. Chem Res Toxicol 18:1462–1470. doi:10.1021/tx0501334

92. Rick SW, Stuart SJ, Berne BJ (1994) Dynamical fluctuating charge force fields : application to liquid water. J Chem Phys 101:6141–6156

93. Rick SW (2001) Simulations of ice and liquid water over a range of temperatures using the fluctuating charge model. J Chem Phys 114:2276–2283. doi:10.1063/1.1336805

94. Rick SW, Berne BJ (1996) Dynamical fluctuating charge force fields: the aqueous solvation of amides. J Am Chem Soc 118:672–679

95. Llanta E, Ando K, Rey R (2001) Fluctuating charge study of polarization effects in chlorinated organic liquids. J Phys Chem B 105:7783–7791

96. Brooks CL, Patel S (2004) CHARMM fluctuating charge force field for proteins: I Parameterization and application to bulk organic liquid simulations. J Comput Chem 25:1–15. doi:10.1002/jcc.10355